Tianjin Daxue Xuebao (Ziran Kexue yu Gongcheng Jishu Ban)/
Journal of Tianjin University Science and Technology
ISSN (Online): 0493-2137
E-Publication: Online Open Access
Vol:55 Issue:01:2022
DOI 10.17605/OSF.IO/U8NVF

NUMERICAL INVESTIGATION OF ULTRASONIC VIBRATION ON THE APPLICATION OF SAC305 ALLOY BY USING FEM APPROACH

KUSSAY AHMED SUBHI, EMAD KAMIL HUSSEIN and HAIDER RAHMAN DAWOOD AL-HAMADANI

Al-Mussaib Technical College TCM, Al-Furat Al-Awsat Technical University ATU,
P.O. Box 51006, Al-Mussaib, Babil, Iraq

ABSTRACT

The recent subject of research in the electronic packaging industry has been technological methods to increase the durability of solder joints. The SAC305 solder joint was used in this research to analyze the mechanical properties of ultrasonic vibration for them. The effect of ultrasonic vibration (USV) respect to range of time within (0sec to 6 sec) on the solder joints properties was characterized systematically. In this study after verification of this computer simulation with experimental results and the results showed it was confidence 87% ,after validation new parameters have been suggested to discover the better mechanical properties for the solder joints and these parameters are deferent range of frequency for specific period of time and substrate material which will be between two plate of copper Cu ,then input all these parameters to ANSYS to analysis the inputs and the output of computer simulation is shear strength . The findings of the numerical analysis revealed that the maximal shear strength for SAC305 alloy was 31.6Mpa when it was eventually treated with 80 kHz for 1.5 sec, this analysis found that the better way to boost mechanical properties for Cu / SAC305 / Cu solder alloy treats this solder joint with frequency 80 kHz for 1.5 sec to achieve optimum shear strength value.

Keywords: ANSYS; FEM; Fractional corrosion; SAC Alloy;USV; Vibration

INTRODUCTION

Today, in the electrical packaging industries, it continues to miniaturize and modern features of mobile products do not minimize the size and weight of electrical packages sufficiently (Bari, 2015). But on the other hand, the system's density is increasing. Therefore, these interconnectors can pass through the output and output of this density (Zhang ET al.2010). The flow allowed the machine to produce heat and this led to a tremendous rise (Fan et al. 2010). The packaging architecture has been designed to improve the characteristics of a thermal built-in, such as increasing the bottom area and promoting it by eliminating unnecessary heat through the thermal direction. (Kim et al. 2011) has showed that, ultrasonic welding is widely used especially in compile the shells of the plastic of an electronic product. Vibration due to ultrasonic has a great effect on solider joints fail om PCB. Fail occurs during the welding process when the structures are not suitable

Tianjin Daxue Xuebao (Ziran Kexue yu Gongcheng Jishu Ban)/
Journal of Tianjin University Science and Technology
ISSN (Online): 0493-2137
E-Publication: Online Open Access
Vol:55 Issue:01:2022
DOI 10.17605/OSF.IO/U8NVF

(Li et al. 2020) have reported that SAC alloys influence all alloy characteristics by the production of intermetallic compounds among the primary elements Sn Ag and Cu. Three intermetallic compounds are probable, which can form: Ag3Sn is formed because of the Sn-Ag reaction and Cu6Sn5 forms due to the reaction of Sn and Cu but Cu3Sn is not formed at the eutectic point until the C content of Cu is high enough to form Cu3Sn in high temperatures. Ag can also react to the process of Ag rich α and Cu rich β. There is, however, no reaction to form any kind of intermetallic compounds between Ag and Cu. The intermetallic particles are much stronger than the bulk material (El-Taher et al. 2020) have reached that the alloys can also be strengthened by fine intermetallic particles in the Sn matrix. Intermetallic compounds can also increase the fatigue life of solders, because the fatigue tolerance of SAC alloys in comparison to SnPb Eutectic solders has shown 3-4 times higher. The greater fatigue resistance, the interspersed Ag3Sn and Cu6Sn5 particles which pin the movement of dislocations and block them are believed to contribute.

In order to simulate solder joint behavior under various circumstances, finite element analysis was widely used. Comparing SnPb and SAC joint reliability with nonlinear SEA in three packages compared silicone, flip and a Package of QFN (Delhaise et al. 2021).

(Ren et al. 2019) have indicated that the SAC rate is lower than in SnPb, but that the lead-free solder was worse when the inelastic energy dissipation was used as a harm parameter for intense loading conditions. This is because the lower shrinkage rate leads to higher pressures and hysteresis and more energy per cycle dissipated. (Ahmed et al. 2020) have employed the procedure of finite element to assess the efficiency of the thermal cycling flip chip kit. The viscoplastic Anand creep and Darveaux creep models were used to consider the solder reaction and fatigue characteristics. In analysis of board level solder joint reliability of thermal cycling BGAs

(Dwivedi et al. 2021) have used the finite element approach along with Anand's creep model. The stability of flip chip solder joints in both matching and rigid substrates, based on the Finite Element and Anand Constituent Model, was modeled.

The leading lead-free solder nominee (95.5Sn3.8Ag0.7Cu) and the 63Sn37Pb solder under thermal cycling were evaluated in (Krishnan et al. 2019) . A research vehicle made up of four 10x10 0.8mm pitch plastic ball grid chained. Arrays (microBGA) mounted on a printed cable board 8 layer FR4 have been produced. The finishing of the board for the Eutectical SnPb instruments was organic solder preservatives (OSP) and HASL (Hot Air Solder) for the plumage free equipment. In rapid cycling of temperature each daisy chain was monitored using an event detector where the test vehicles were cycled at a ramp pace of about 3oC a minute from –40oC to 125oC with 10-minute stays and 2 hours 10 minutes in total. The results shown by a Weibull distribution have shown that, under these circumstances, the solder SAC is more durable. They conducted experiments on big, plomb-free solder samples to determine the required parameters for the viscoplasticity model of Anand. In a final factor analysis using ANSYS®, the Anand model was then used in order to evaluate viscoplastic work for each solder joint along the package diagonal, through means of a submodeling

Tianjin Daxue Xuebao (Ziran Kexue yu Gongcheng Jishu Ban)/
Journal of Tianjin University Science and Technology
ISSN (Online): 0493-2137
E-Publication: Online Open Access
Vol:55 Issue:01:2022
DOI 10.17605/OSF.IO/U8NVF

technique. Tests of stress levels. Afterwards, you will check some of the jobs. The leadfree solder material 95.5Sn3.9Ag0.6Cu was studied by (Erer et al. 2018). The effects of strain rate in SAC solder were studied at room temperature on hysteresis loops and fatigue life. They defined the isothermal tiredness of the material with a criterion of fatigue failure based on the principle of damage accumulation in solder material using the theory of damage mechanics. The model has been tested with experimental evidence, and it has been shown that it can determine how fatigue and cyclical behavior can affect load rates. To have full understanding of the underlying behaviment of the harm dynamics, the impact of temperature and microstructure was required. In a sequence of as-soldered, thermal-aging, copper/lead-free soil joints, both monotonous and cyclically deformed.

According to (Shakil et al.2014), the enhanced simulation has become an acceptable choice to test problems with solder joints in terms of failure due to ultrasonic vibration welding . Based on the study of (Lee et al. 2013), the FEM was performed during the welding process to research the dynamic vibration process. Many researchers such (Nanu et al. 2011) have mentioned that FE techniques have been developed to predict the damage caused by ultrasonic welding in the plastic component. Numerical models of thin metal with ultrasonic vibration have also been suggested for many applications In terms of mechanical properties in the top foil and substrate (Ranim, 2013;Liu et al. 2015) have a great contribution in a FEM to illustrate ultrasonic welding .

Since cost plays a very important rule in any architecture, (Sackmann et al. 2015; Annoni, 2011) have discovered the small finite element model regime to analyze the failure of the elements but still face some structure geometry difficulties. Therefore, this study will concentrate on efficient FE analysis and will allow us to develop solder joint mechanical properties and to investigate better property properties.

MATERIALS AND METHODS

The summarized methodology process of the research can be mentioned as following: The initial stage for beginning the analysis is to describe the problem statement of the study based on details given in the flow map. A literature review must be carried out in order to accomplish the goals of the report.

Usually, software will select a software to do the simulation process, depending on the field of study. ANSYS program was selected to conduct the simulation process in this report.

Finite Element Analysis set up

In this analysis, the Finite Element analysis was performed statically, modally, and transitionally. The normal frequencies and model shapes of the equipment are determined by modal analysis. Natural frequencies and design forms are major feature parameters for conditions of dynamic loading. The resonating frequencies and fashion forms determine alloy structure stability. The computer which experience unregulated

Tianjin Daxue Xuebao (Ziran Kexue yu Gongcheng Jishu Ban)/
Journal of Tianjin University Science and Technology
ISSN (Online): 0493-2137
E-Publication: Online Open Access
Vol:55 Issue:01:2022
DOI 10.17605/OSF.IO/U8NVF

non-linear deformity if the frequency expected by the model is similar to or at a resonant frequency, which can contribute to a system failure or misleading test results.

Geometry and Meshing

The research samples included a soldering paste of the type Sn-3.0Ag -0.5Cu(SAC 305) and two substrates of copper(Cu), measuring 15 mm x 15 mm, 3 mm and 2 mm x 8 mm diameter for the upper substrate . The surface of the substrates was ground, polished and washed until soldering with normal metallographic techniques. A mask with opening diameter of 6 mm and 0.4 mm in thickness deposited then the SAC305 paste among the substrates (equivalent to 0.1 g of solder paste). Figure 1 illustrates the structure of the test sample

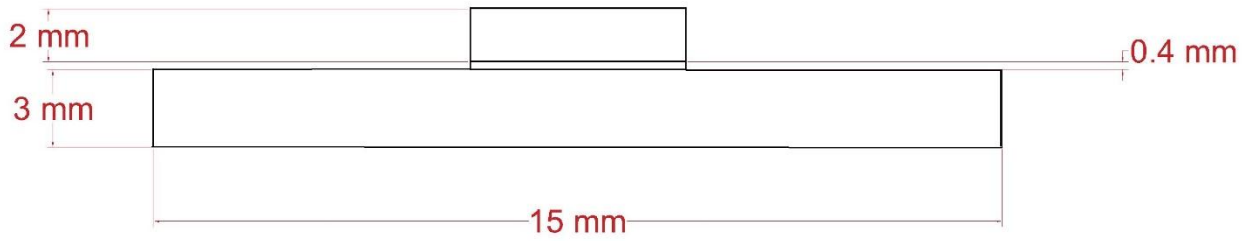

Figure 1. Geometry (structure) of test sample (Side view)

In this research AUTOCA software has been conducted to produce the geometry of the project. Mesh has been generated by using ANSYS mechanical and that was based on the study of (Tan et al. 2017). Tri type pave mesh has been employed in complicated meshed model and quad type was employed in the rest meshed model.as shown in figure 2 ANSYS provide a completed mesh

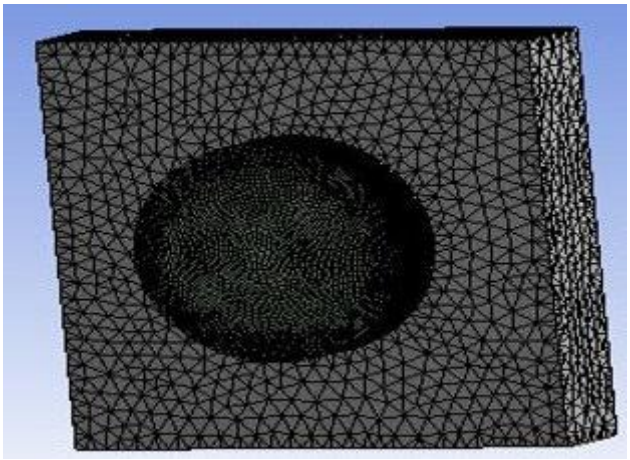

Figure 2. The meshing model

Tianjin Daxue Xuebao (Ziran Kexue yu Gongcheng Jishu Ban)/
Journal of Tianjin University Science and Technology
ISSN (Online): 0493-2137
E-Publication: Online Open Access
Vol:55 Issue:01:2022
DOI 10.17605/OSF.IO/U8NVF

Boundary Conditions

In this research, SAC alloy was carried out to investigate the characters of this alloy within a particular period due to high frequencies. The following table shows the SAC alloy features.

Table .1 Mechanical properties of SAC305 alloy

SAC Alloy	Solidus C	Liquidus C	Density gm/cm^3	Young's Modulus of elasticity GPA
	217	220	7.4	16.6

RESULTS AND DISCUSSION

Convergence tests

SAC alloy has been conducted as preprocessing in ANSYS 16.1 using vibration response tool .in this research meshed model has been created locally. The current type of elements is satisfied with linear loads .As shown in figure 3 seven solutions with different number of elements have been conducted with same applied load 500 N and the out put with a total deflection . Based on the results that has been collected from simulation. the curve of become horizontal at 0.10 mm (total deflection)with a 10,064 elements. This test has proven that the meshed model is converged.

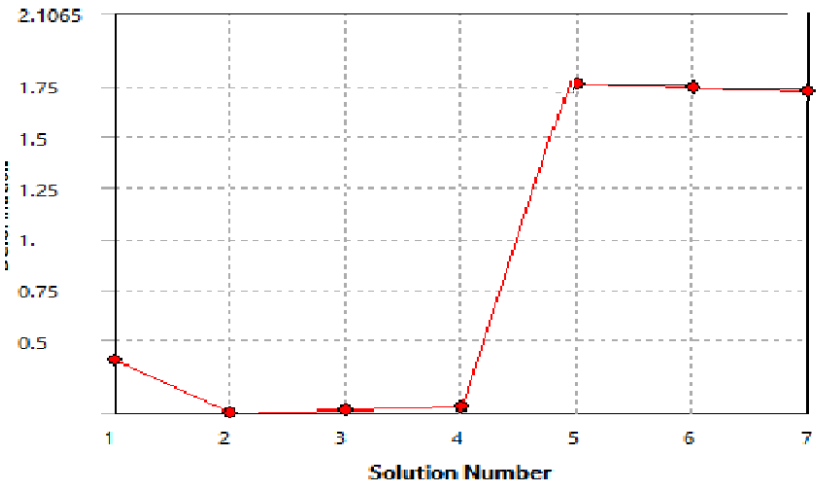

Figure .3 Convergence test of the SAC alloy model in terms of Total Deflection

Tianjin Daxue Xuebao (Ziran Kexue yu Gongcheng Jishu Ban)/
Journal of Tianjin University Science and Technology
ISSN (Online): 0493-2137
E-Publication: Online Open Access
Vol:55 Issue:01:2022
DOI 10.17605/OSF.IO/U8NVF

Validation

In order to continue with the current boundary conditions, the validation process should be carried out under the same boundary conditions as the experimental work carried out .The simulation method is carried out in order to have the findings seen in Figure 4. The relation between the experimental simulation and the effects of the simulation as seen in Figure 4. In this analysis, the findings were 87 percent conviction after verification of this computer simulation with experimental results.

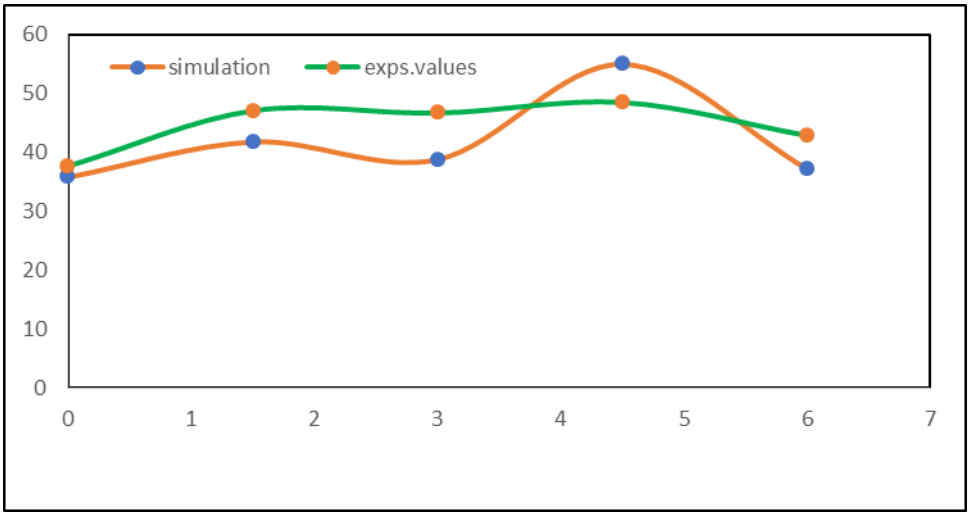

Figure 4. Comparison between simulation results and experiment results

Response to vibration

The numerical results have revealed that the response of the SAC alloy to the vibration in terms of amplitude (stress) is vary. This analysis has been conducted using Harmonic Response tool in ANSYS software. In this research, Amplitude (stress) has been considered as main indicator for the vibration response of SAC alloy. Figure 5. Shows that the maximum amplitude is began at applied frequency 40 Hz and suddenly to sharp decreasing at 45 Hz. The minimum amplitude has been occurring after sharp decreasing at 200 Hz. Another maximum value of amplitude happened at 340 Hz. The benefit of this test is to understand mechanical behavior of material to the applied frequencies. thus, for the used material (SAC alloy) the vibration response is not stable.

Tianjin Daxue Xuebao (Ziran Kexue yu Gongcheng Jishu Ban)/
Journal of Tianjin University Science and Technology
ISSN (Online): 0493-2137
E-Publication: Online Open Access
Vol:55 Issue:01:2022
DOI 10.17605/OSF.IO/U8NVF

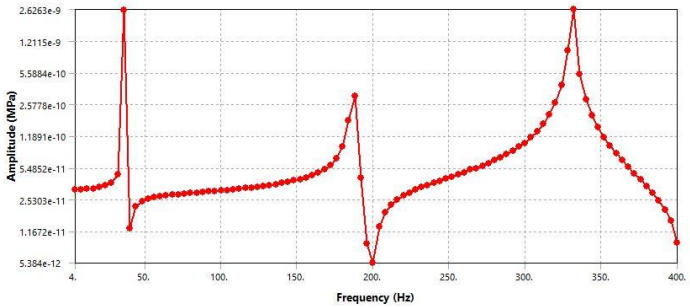

Figure 5. Vibration response in terms of Amplitude (MPa)

Implementation of New Range Frequency

In this study high values of frequency with a specific time of flow has been conducted in order to characterize solider joint in term of shear strength. Thus 80 KHz and 90 KHz of frequencies are employed to be investigated.

Implementation of 80 Khz

ANSYS software has been conducted to simulate the shear strength of SAC350 alloy due to the specific range of time of flow. Figure 6 shows the result that has been gotten by using FE model

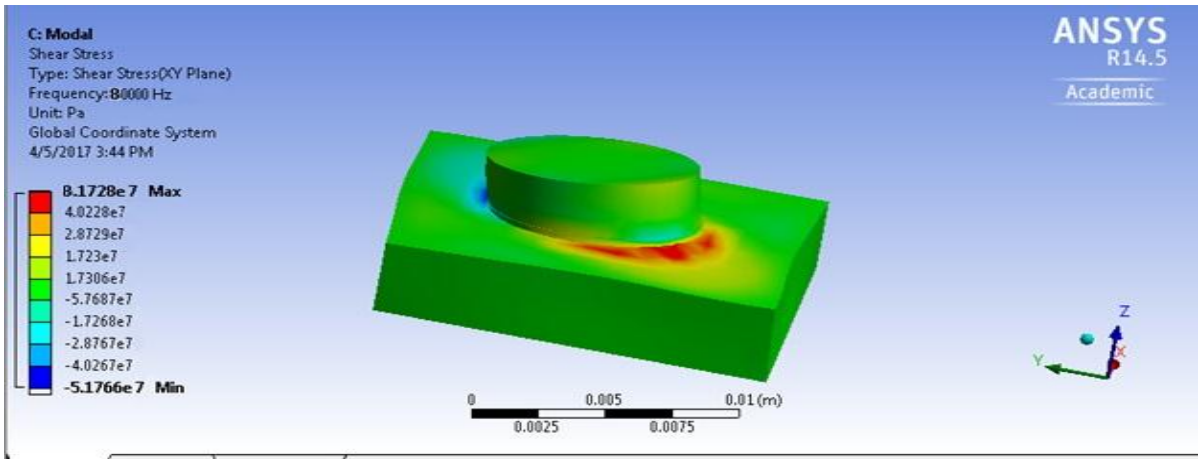

Figure 6. The graphical effect on the SAC alloy due high frequency (80 Khz)

The 80 kHz frequency was used in this trial with a flow time interval of six (0,1.5,3,4.5,6 sec). At 1.5 sec, the max performance (force) was 31.6 MPa. As well as the results, it was shown that the lowest output occurred at the highest flow time as flow 22.09 MPa at 6 sec. Figure 6 indicates the frequency implementation for a different time span as shown in figure 7.

Tianjin Daxue Xuebao (Ziran Kexue yu Gongcheng Jishu Ban)/
Journal of Tianjin University Science and Technology
ISSN (Online): 0493-2137
E-Publication: Online Open Access
Vol:55 Issue:01:2022
DOI 10.17605/OSF.IO/U8NVF

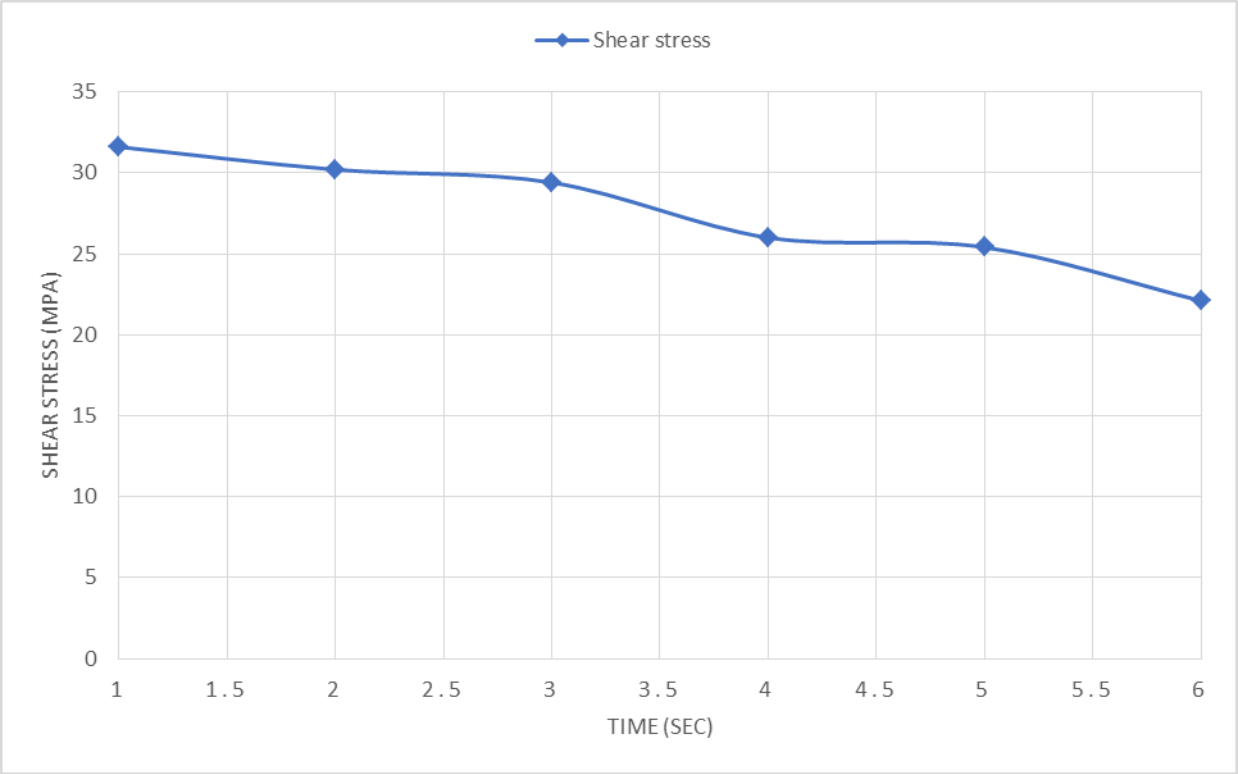

Figure 7. Shear strength with time of 80 khz

Implementation of 90 Khz

Figure 8 shows the graphical effect of vibration on SAC alloy in terms of shear stress. Where the two substants subjected to horizontal (Y direction) forces that lead to shear stress. The force has been applied with organized range of frequency. These investigation was carried out by applying 90 Khz

Tianjin Daxue Xuebao (Ziran Kexue yu Gongcheng Jishu Ban)/
Journal of Tianjin University Science and Technology
ISSN (Online): 0493-2137
E-Publication: Online Open Access
Vol:55 Issue:01:2022
DOI 10.17605/OSF.IO/U8NVF

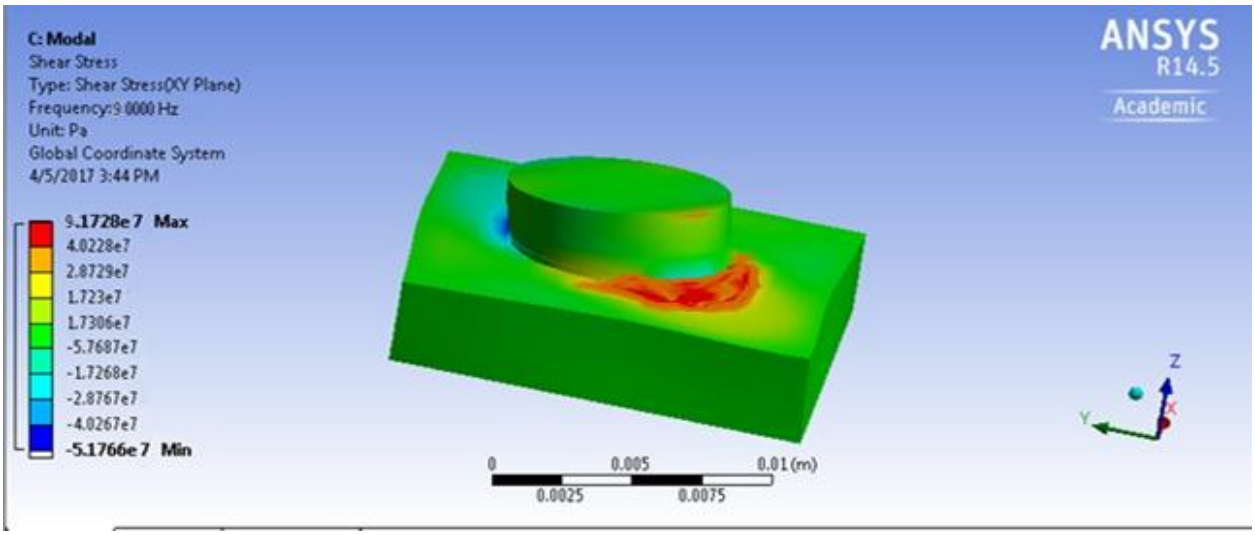

Figure 8. The graphical effect on the SAC alloy due high frequency (90 Khz)

The numerical results have stated that, 90 kHz frequency was used in this trial with a flow time interval of six (0,1.5,3,4.5,6 sec). At 1.5 sec, the max performance (force) was 32.56 Mpa . As well as the results, it was shown that the lowest output occurred at the highest flow time as flow 24.9 MPa at 6 sec. Figure 6 indicates the frequency implementation for a different time span as shown in figure 9.

Tianjin Daxue Xuebao (Ziran Kexue yu Gongcheng Jishu Ban)/
Journal of Tianjin University Science and Technology
ISSN (Online): 0493-2137
E-Publication: Online Open Access
Vol:55 Issue:01:2022
DOI 10.17605/OSF.IO/U8NVF

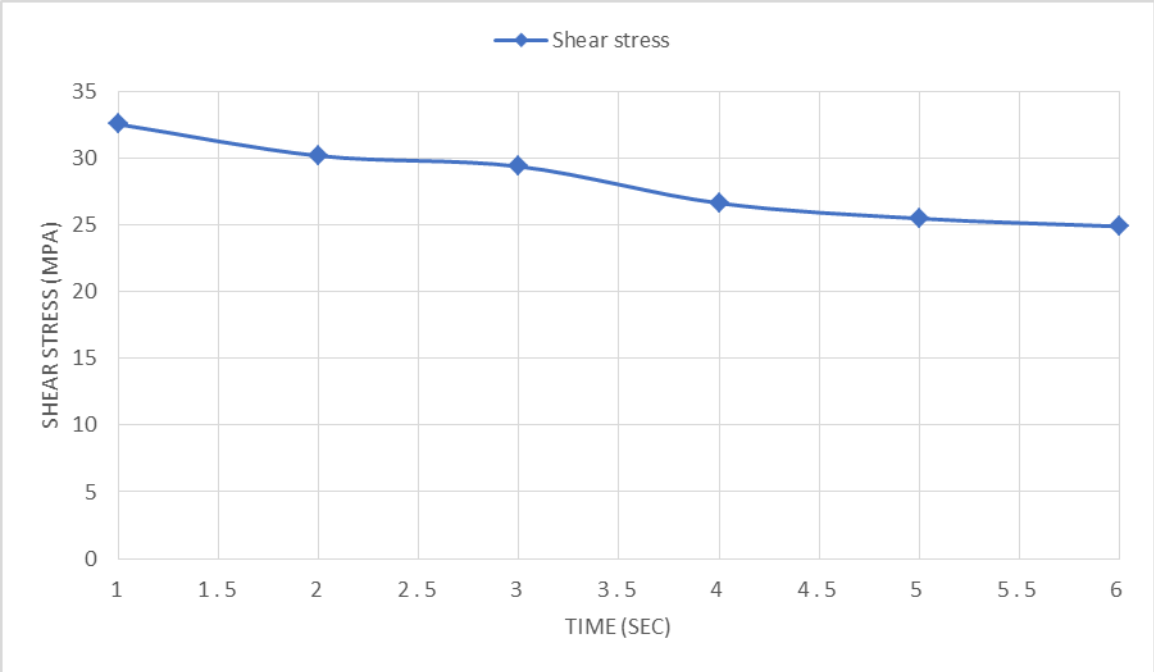

Figure 9. Shear strength with time of 90 khz

The findings that were achieved by simulation are seen in figure 6. The graph shows that owing to two frequencies, 90 kHz and 80 kHz, the two curves are. According to the results given by the simulation, the intensity values attributable to 90 kHz are greater than the results obtained by 80 kHz at the same interval.

CONCLUSION

For cu / sac / cu solder alloy to assess the higher shear strength than the test sample when handled with deferential ultrasonic vibration values. The sample was treated according to the time intervals (0, 1.5, 3, 4.5, 6sec) of the UV ultrasonic vibration time to investigate that the result indicated shear intensity for Cu / SAC305 / Cu when the frequency was 80 kHz with a 6 flow time interval (0,1.5,3,4.5,6 sec). The maximum output at 1.5 sec (shear strength) was 31.6 MPa. In addition, the results showed that the minimum output occurred at 6 sec at the highest flow time of 24.09 MPa. But the maximum strength of the Cu / SAC305 / Cu alloy was achieved at 32.56 Mpa at 1.5 sec in the case of 90 KHz, with the same boundary conditions. The minimum strength is 24.9 MPa. It occurred at a 6 sec maximum flow time.

Tianjin Daxue Xuebao (Ziran Kexue yu Gongcheng Jishu Ban)/
Journal of Tianjin University Science and Technology
ISSN (Online): 0493-2137
E-Publication: Online Open Access
Vol:55 Issue:01:2022
DOI 10.17605/OSF.IO/U8NVF

REFERENCES

1. Baïri, A. (2015). Thermal design of tilted electronic assembly with active QFN16 package subjected to natural convection. *International Communications in Heat and Mass Transfer*, *66*, 240-245.
2. El-Taher, A. M., Abd El Azeem, S. E., & Ibrahiem, A. A. (2020). Influence of permanent magnet stirring on dendrite morphological and elastic properties of a novel Sn–Ag–Cu–Sb–Al solder alloy by ultrasonic pulse echo method. Journal of Materials Science: Materials in Electronics, 31(12), 9630-9640.
3. Erer, A. M., Oguz, S., & Türen, Y. (2018). Influence of bismuth (Bi) addition on wetting characteristics of Sn-3Ag-0.5 Cu solder alloy on Cu substrate. Engineering Science and Technology, an International Journal, 21(6), 1159-1163.
4. Krishnan, P. K., Christy, J. V., Arunachalam, R., Mourad, A. H. I., Muraliraja, R., Al-Maharbi, M., ... & Chandra, M. M. (2019). Production of aluminum alloy-based metal matrix composites using scrap aluminum alloy and waste materials: Influence on microstructure and mechanical properties. Journal of Alloys and Compounds, 784, 1047-1061.
5. Dwivedi, S. P., Saxena, A., Sharma, S., Srivastava, A. K., & Maurya, N. K. (2021). Influence of SAC and eggshell addition in the physical, mechanical and thermal behaviour of Cr reinforced aluminium based composite. International Journal of Cast Metals Research, 34(1), 43-55.
6. Ahmed, S., Suhling, J. C., & Lall, P. (2017, May). The anand parameters of aging resistant doped solder alloys. In 2017 16th IEEE Intersociety Conference on Thermal and Thermomechanical Phenomena in Electronic Systems (ITherm) (pp. 1416-1424). IEEE.
7. Ren, G., & Collins, M. N. (2019). Improved reliability and mechanical performance of Ag microalloyed Sn58Bi solder alloys. Metals, 9(4), 462.
8. Delhaise, A. M., Bagheri, Z., Meschter, S., Snugovsky, P., & Kennedy, J. (2021). Tin Whisker Growth on Electronic Assemblies Soldered with Bi-Containing, Pb-Free Alloys. Journal of Electronic Materials, 50(3), 842-854.
9. Zhang, H. Y., Mui, Y. C., & Tarin, M. (2010). Analysis of thermoelectric cooler performance for high power electronic packages. *Applied thermal engineering*, *30*(6-7), 561-568.
10. Fan, X. J., Varia, B., & Han, Q. (2010). Design and optimization of thermo-mechanical reliability in wafer level packaging. *Microelectronics Reliability*, *50*(4), 536-546.
11. Kim, T. H., Yum, J., Hu, S. J., Spicer, J. P., & Abell, J. A. (2011). Process robustness of single lap ultrasonic welding of thin, dissimilar materials. *CIRP annals*, *60*(1), 17-20.
12. Shakil, M., Tariq, N. H., Ahmad, M., Choudhary, M. A., Akhter, J. I., & Babu, S. S. (2014). Effect of ultrasonic welding parameters on microstructure and mechanical properties of dissimilar joints. *Materials & Design*, *55*, 263-273.
13. Lee, D., Kannatey-Asibu, E., & Cai, W. (2013). Ultrasonic welding simulations for multiple layers of lithium-ion battery tabs. *Journal of Manufacturing Science and Engineering*, *135*(6), 061011.
14. Nanu, A. S., Marinescu, N. I., & Ghiculescu, D. (2011). Study on ultrasonic stepped horn geometry design and FEM simulation. *Nonconventional Technologies Review*, *4*, 25-30.
15. Rani, M. R., & Rudramoorthy, R. (2013). Computational modeling and experimental studies of the dynamic performance of ultrasonic horn profiles used in plastic welding. *Ultrasonics*, *53*(3), 763-772.
16. Liu, X., Wu, C., & Padhy, G. K. (2015). Characterization of plastic deformation and material flow in ultrasonic vibration enhanced friction stir welding. *Scripta Materialia*, *102*, 95-98.
17. Li, F., Verdingovas, V., Dirscherl, K., Harsányi, G., Medgyes, B., & Ambat, R. (2020). Influence of Ni, Bi, and Sb additives on the microstructure and the corrosion behavior of Sn–Ag–Cu solder alloys. Journal of Materials Science: Materials in Electronics, 31(18), 15308-15321.
18. Sackmann, J., Burlage, K., Gerhardy, C., Memering, B., Liao, S., & Schomburg, W. K. (2015). Review on ultrasonic fabrication of polymer micro devices. *Ultrasonics*, *56*, 189-200.
19. Annoni, M., & Carboni, M. (2011). Ultrasonic metal welding of AA 6022-T4 lap joints: Part I–Technological characterisation and static mechanical behaviour. *Science and Technology of Welding and Joining*, *16*(2), 107-115.
20. Tan, A. T., Tan, A. W., & Yusof, F. (2017). Effect of ultrasonic vibration time on the Cu/Sn-Ag-Cu/Cu joint soldered by low-power-high-frequency ultrasonic-assisted reflow soldering. *Ultrasonics sonochemistry*, *34*, 616-625.